Neural Network Comparing Two Rate-Encoded Inputs Entering in Parallel

J. PAVLÁSEK AND T. HROMÁDKA

Institute of Normal and Pathological Physiology, Slovak Academy of Sciences, Bratislava, Slovakia

Abstract. Presented computational model of a neural network is able to compare two regular input frequencies. The comparison is based on detection of inter-spike interval differences of the two frequencies. This detection is continuous and the network dynamically changes its output according to the changes in the input frequencies. The entire network is composed of biologically plausible parts. A combination of such simple comparators might be involved in the information processing in the central nervous system.

Key words: Rate coding — Frequency coding — Neural network — Decoding

Introduction

The sensory system provides an organism with a continuous representation of internal and external environments. The different types of stimuli are transformed into a change of a membrane potential of peripheral receptors and neurons that – when exceeding the threshold, leads to generation of action potentials (spikes). The spike trains then bring the information about the sensory stimuli into the CNS.

Thus the physical parameters of stimuli are *encoded* into spike trains which are considered to be binary strings *representing* biologically significant symbols within the particular context being investigated. The minimum set of symbols capable of representing all of the biologically significant information about the stimulus defines *a neural code* (Theunissen and Miller 1995).

Many encoding schemes have been considered by neurobiologists so far and the process of encoding is still not completely understood. However, it is generally accepted that, when encoding in a temporal domain, the two main types of neural codes are *temporal* code and *rate* code (Theunissen and Miller 1995; Gerstner et al. 1997). In the temporal encoding scheme, the relevant information is correlated with the *timing* of the spikes within an encoding window (Richmond et al. 1987, 1990; McClurkin et al. 1991; Pavlásek 1999). In the (mean) rate encoding scheme,

Correspondence to: Doc. MUDr. Juraj Pavlásek, DrSc., Institute of Normal and Pathological Physiology, Slovak Academy of Sciences, Vlárska 5, 833 34 Bratislava, Slovakia. E-mail: unpfpavl@savba.sk

the relevant information encoded about the stimulus is correlated only with the *number* of elicited spikes within the (temporal) encoding window (Konishi 1991; Hsiao et al. 1993).

The processing of the rate encoded inputs in central nervous system may reflect two different situations and each of them requires different mechanisms of rate "decoding".

One situation occurs when the rate encoded inputs enter the network sequentially. Such situation (stimulus 1-pause-stimulus 2) dealing with vibratory tactile stimuli was considered in Mountcastle et al. (1990); Hernández et al. (2000). The detection of these stimuli and differentiation of their frequencies requires "decoding" mechanisms capable of discerning between the spike trains transmitted sequentially in the same information channel and the memory mechanisms storing the information about the first and the second stimuli.

Another situation is suggested when the continuous comparison of frequencies incoming in parallel from various places of activated receptor sheet is necessary for sensory processing. To process this type of neural code, mechanisms able to compute differences in firing rate (frequencies) in a sensory channel might be assumed (Hsiao et al. 1993).

The specific nature of the rate encoding scheme has significant implications for biologically relevant "decoding" mechanisms. The "decoding" scheme may use the mechanism of spatio-temporal summation based on convergence. However, for lower frequencies, taking into account the duration of postsynaptic potentials, the spatio-temporal summation cannot be sufficient.

In this paper we focus on the problem of comparing two rate encoded inputs entering simultaneously the neural network model. The network proposed must be able to compare the simultaneously incoming frequencies and to recognize the difference between them. The input frequencies are supposed to be within the range of 20–100 Hz, which is in the frequency range used for information transmission in the central nervous system (Willis and Coggeshall 1991); i.e. the network must be also able to process the spike trains with interspike intervals 10–50 ms. The difference in the input frequencies, if any, should be signalled in spiking activity at the output. Both outputs should remain silent if the input frequencies are the same.

Methods

The computer model JASTAP obeys the principles concerning the physiology of a biologically realistic neuron with chemical transmission of information. Details of the model have been reported elsewhere (Jančo et al. 1994). Herein, we only give a brief account of the essential properties used in the simulations shown in this paper.

The basic element of the network is a model neuron (neuroid) behaving as an integrate-and-fire element. It is described by:

1. Instantaneous membrane potential (Mp). Mp is a dimensionless quantity within the range $\langle -1, 1 \rangle$.
2. Membrane potential determined as the sum of postsynaptic potentials (Psp) limited by the nonlinear function

$$Mp(t) = (2/\pi) \arctan\left(\sum Psp(t)\right) \tag{1}$$

3. A threshold (Th) from the interval $\langle 0, 1 \rangle$.
4. The frequency of spikes (Sp) is restricted by the absolute refractory period. This is managed by setting minimum (I_{mn}) and maximum (I_{mx}) interspike intervals. The actual interspike interval (I_a) is determined as

$$I_a = I_{mn} + (I_{mx} - I_{mn})(2/\pi) \arctan((Mp - Th)/(1 - Mp)) \tag{2}$$

   The standard value for I_{mn} was 1 ms, and I_{mx} ranged from 2 ms to 10 ms. The relative value of Th was set to 0.5 for all neuroids.
5. Behaviour in terms of phasicity or tonicity (these functions were not activated in the present work). Every neuroid can have 8 synaptic inputs but only a single output. The program treats the synapse as a part of the neuroid. The output can be connected to one or several synapses in the network of neuroids. A synapse is characterized by:
   a) The input connected to it.
   b) The shape of a Psp prototype, which is evoked by Sp arriving at this synapse (the particular waveform is selected from a set of prototype Psp shapes stored in a buffer of Psp waveforms). The Psp prototype is described by

$$Psp(t) = k(1 - \exp(-t/t_1))^2 \exp(-2t/t_2) \tag{3}$$

      The waveform simulates whether the synapse in question is located on the soma or on the dendritic tree (the time-course and the attenuation of its amplitude). In this presentation uniform Psp time-courses (Fig. 2B) were used, one for excitatory and another for inhibitory Psp. Experimental data are best simulated with parameters $t_1 = 0.3$ ms and $t_2 = 2.7$ ms.
   c) The latency (time delay) of the synaptic transmission and/or axonal conduction.
   d) The synaptic weight (Sw) has its value from the interval $\langle -1, 1 \rangle$. Sw simulates effectiveness of a synaptic input (a synchronously activated set of axons of the same type or a cluster of the terminal branches of an axon).
   e) Developmental changes which determine instantaneous, effective Sw. These mechanisms representing plastic activity-induced alterations were not activated in presented simulations.

The computer program JASTAP has been written in C++ language. The program can define a network by simple command language and simulate its activity in discrete time intervals (0.5 ms steps). Samples of simulated activity are presented in the form of intracellular recording with a microelectrode, or as a raster map of the spike potentials.

Results

Notation and conventions

In simulation experiments (see below) we used regular input frequencies $F^{(1)}$, $F^{(2)}$ (Fig 1A) of 20–100 Hz To describe the input frequencies we used the following notation conventions (Fig 1B,C) The sequence of spikes can be considered to be a train of discrete impulses $\{SP_i\}$ Because we assumed regular input frequencies the interspike interval lengths were constant inside a given time window – it was possible to describe each train of impulses as $SP_k = SP_0 + kI$, where SP_0 is the spike arrival time of the first spike (in ms), I is the inter-spike interval (in ms), and $k = 1, 2, 3, 4,$ We used the superscripts $^{(1)}$ and $^{(2)}$ to distinguish between the two input spike trains entering *via* $INP1$ or $INP2$ respectively

To describe the relations between two input frequencies we denoted the difference between the first spike arrival times by $D = SP_0^{(1)} - SP_0^{(2)}$ and the inter-spike

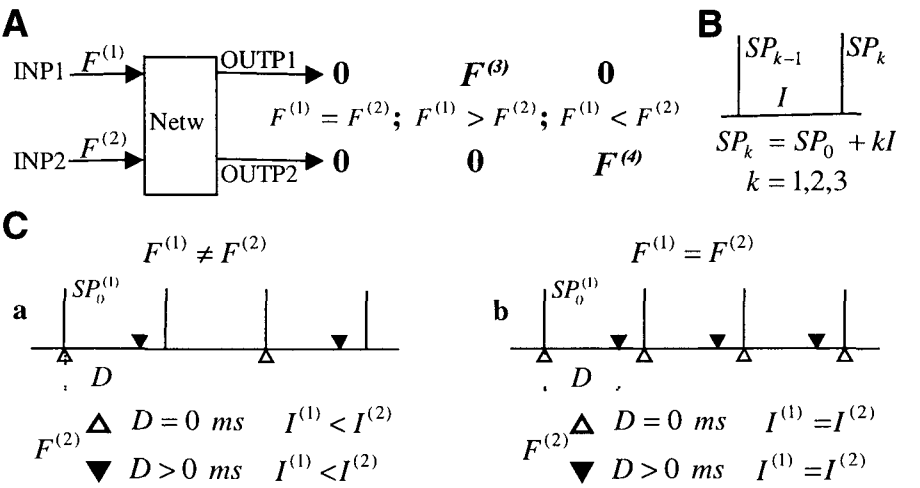

Figure 1. Definition of the problem **A.** A proposed relation among input and output frequencies The input frequencies ($F^{(1)}$, $F^{(2)}$) enter the network (Netw) *via* $INP1$ or $INP2$ respectively If the frequencies are equal the outputs are silent if $F^{(1)} > F^{(2)}$ ($F^{(2)} > F^{(1)}$) then $OUTP1$ ($OUTP2$) is active, the output frequency is denoted by $F^{(3)}$ ($F^{(4)}$) **B.** A schematic description of the spike train where I denotes the inter-spike interval length and SP_k denote the time of spike occurrence **C.** Relations between $F^{(1)}$ (vertical bars) and $F^{(2)}$ (triangles) $SP_0^{(1)}$ is the first spike of $F^{(1)}$, D denotes the difference in the first spike arrival times of $F^{(1)}$ and $F^{(2)}$ a) The two input frequencies are unequal The situation where $F^{(1)} > F^{(2)}$ ($I^{(1)} < I^{(2)}$) is shown The frequencies can start either simultaneously (vertical lines *vs* empty triangles) or non-simultaneously (vertical lines *vs* black triangles), b) The two input frequencies are equal ($F^{(1)} = F^{(2)}$) Again, the frequencies can start either simultaneously (empty triangles) or non-simultaneously (black triangles)

interval difference between two input frequencies by $\Delta I = |I^{(1)} - I^{(2)}|$. Full description of the input spike trains is then given by $SP_0^{(1)}$ (the first spike arrival time of the first input) or $SP_0^{(2)}$, difference D and the lengths of inter-spike intervals $I^{(1)}$ and $I^{(2)}$. To simplify the morphological and functional description (see below) of the network we use the terms *network channel* and *side of the network*. Two parallel network channels (sides of the network) are involved in processing of different inputs; $F^{(1)}$ channel includes neuroids $nn.0, 1, 2, 3, 9$, $F^{(2)}$ channel includes $nn.4, 5, 6, 7, 10$ (Fig. 2A). The $n.8$ is shared by both inputs and channels.

The approach to problem solution

The main principle underlying the presented solution is a continuous concurrency of the opposite sides of the network in creation of a time window. The time window is a time period during which one side of the network is ready to create an output and it is, in fact, an inter-spike interval of the corresponding input frequency.

If two spikes enter the network simultaneously *via* both inputs ($INP1$ and $INP2$) the propagated activity in both channels – except the output neuroids – is stopped.

Non-simultaneous spikes entering the network inhibit the activity of the opposite side of the network ("capture" the time window from the opposite side) and start a reverberatory activity in oscillatory circuit ("create" the time window) persisting during the time window duration.

While "holding" the time window the particular side of the network is ready to create an output activity. If another spike enters the network *via* the same input during this period, the corresponding output neuroid generates propagated signal. Thus an output is generated if two successive spikes of one input stream enter the network *between* two successive spikes of the other stream.

For example, let us assume that $F^{(1)}$ is higher than $F^{(2)}$ (Fig. 1Ca). This means that $I^{(1)}$ is shorter than $I^{(2)}$. In this case, after some time, two successive spikes of $F^{(1)}$ must necessarily enter the network *between* two successive spikes of $F^{(2)}$ and the $F^{(1)}$ channel "captures" the time window. Consequently the inputs (monosynaptic, polysynaptic) of output neuroid ($n.3$ in this case) are activated and the output neuroid generates a spike.

This is the situation shown in Fig. 1Ca. If the black triangles show the position of $F^{(2)}$ spikes then the second and third spikes of $F^{(1)}$ are inside the first inter-spike interval of $F^{(2)}$. Consequently – after arrival of the third $F^{(1)}$ spike – the output neuroid 3 generates a propagated signal.

The model network

Network connectivity

The model network (Fig. 2A) consists of 11 neuroids. Two inputs ($INP1$ and $INP2$) diverge into three branches each, establishing monosynaptic connections with: a) $n.8$.; b) output neuroids 3 ($INP1$) or 7 ($INP2$); and c) input neuroids 0 ($INP1$) or $n.4$ ($INP2$).

Convergent inputs $INP1$, $INP2$ making connections with n 8 form subthreshold excitatory synapses The divergent output connections of n 8 form inhibitory synapses with the first three neuroids of each channel (nn 0, 1, 2 from one side of the network and nn 4, 5, 6 from the other one)

The monosynaptic connections between the inputs and the appropriate output neuroids ($INP1 - n$ 3, $INP2 - n$ 7) have excitatory subthreshold influence

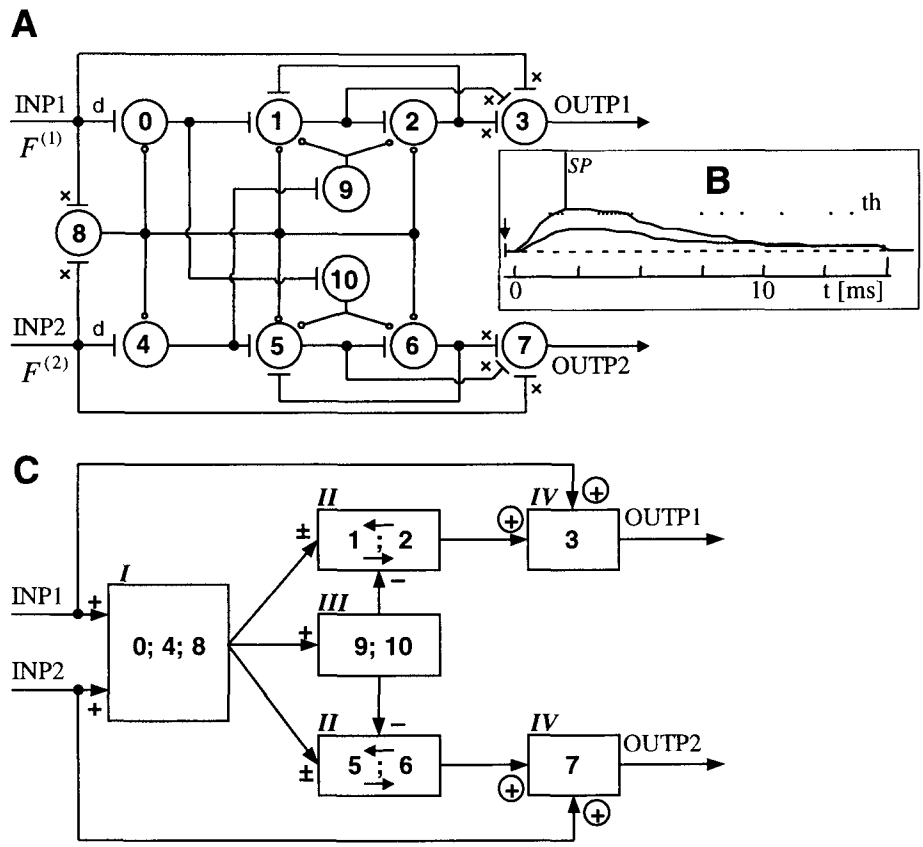

Figure 2. The model neural network **A.** The model network consisting of 11 model neurons (neuroids 0–10), two inputs ($INP1$, $INP2$) and two outputs ($OUTP1$, $OUTP2$) Connections marked by bars (dots) are excitatory (inhibitory), crosses indicate subthreshold excitatory influence, d indicates a delay line **B.** Time courses of postsynaptic potentials used in the model neuron Sub-threshold and supra-threshold (with the resulting spike SP) post-synaptic potentials are shown The dash-dot-dot horizontal line represents the resting membrane potential, the dotted line represents the threshold (th) The start of stimulus which elicited the postsynaptic potentials is marked by the arrow **C.** Main functional blocks of the network All neuroids (0–10) are grouped into 4 functional blocks (I-IV) Arrows show the activity flow, connections marked by pluses (minuses) are excitatory (inhibitory), encircled pluses indicate subthreshold excitatory influence

Polysynaptic pathway in each network channel is composed of four neuroids connected in series ($nn.0-1-2-3$ or $nn.4-5-6-7$). The efferent connection of input neuroid ($n.0/n.4$) diverges and makes synaptic contact with an inhibitory neuroid ($n.10/n.9$) from the other side of the network. These connections are the only functional contacts between the channels. The diverging outputs of inhibitory neuroids ($n.10/n.9$) form inhibitory synapses with $nn.5,6/nn.1,2$.

Second and third neuroids in each channel ($nn.1,2$ and $nn.5,6$) have reciprocal excitatory connections forming a closed loop. Outputs of these neuroids converge on the output neuroid ($n.3/n.7$) and form subthreshold excitatory synapses together with monosynaptic subthreshold excitatory influence from $INP1$ or $INP2$.

Main functional blocks

Each input frequency ($F^{(1)}$ or $F^{(2)}$) (Fig. 1A) enters the network *via* its own input ($INP1$ or $INP2$) (Fig. 2A). The activity of $OUTP1$ and $OUTP2$ depends on the relation between $F^{(1)}$ and $F^{(2)}$. If compared frequencies are the same – whether simultaneous ($D = 0$ ms) or not ($D \neq 0$ ms) (Fig. 1Cb) – both outputs remain silent. If $F^{(1)}$ and $F^{(2)}$ are unequal, only the output of the channel processing higher input frequency is activated.

The neuroids are grouped into 4 functionally different blocks (Fig. 2C).

1. The first (input) block (I) has two main functions. Neuroid 8 serves as a coincidence detector and detects the simultaneously entering spikes. If such spikes are detected $n.8$ blocks the input at the level of $nn.0,4$ and resets the oscillatory circuits [$n.1-n.2$] and [$n.5-n.6$]. Neuroids 0 and 4 activate the oscillatory circuits ([$n.1-n.2$] or [$n.5-n.6$]) and the inhibitory block ([$n.9$; $n.10$]).
2. The oscillatory circuits (II) [$n.1-n.2$] and [$n.5-n.6$] serve as dynamic memories. They receive the inputs from previous (input) block (I, $nn.0,4$). Each spike arriving from the input block starts a reverberatory activity in appropriate circuit which means that the channel is currently holding the time window. This activity continuously stimulates (sub-threshold intensity) the output neuroid ($n.3$ or $n.7$) and prepares it for generation of output signal.
3. Once activated, the reverberatory activity can be stopped only from the opposite side of the network *via* the activity of inhibitory block (III) [$n.9$; $n.10$] (memory reset).
4. The output blocks (IV) [3] and [7] receive two inputs.
   a) Activity transmitted monosynaptically from the corresponding input ($INP1$ or $INP2$).
   b) Activity provided by the corresponding dynamic memory ([$n.1-n.2$] or [$n.5-n.6$]).

Both inputs excite the output neuroids with subthreshold intensity, thus the suprathreshold activation of output neuroid ($n.3$ or $n.7$) requires coactivation of both inputs.

Activity flow

Every spike entering the network (Fig 2A,C) is a) transmitted directly to the corresponding output block (IV) and b) processed in the input block (I)

In the input block the spikes are transmitted to a coincidence detector (n 8) which eliminates all spikes entering the network simultaneously If simultaneous spikes are detected, n 8 inhibits the propagated activity in the network ("resets" the network)

Non-simultaneous spikes transmitted monosynaptically to n 0 ($INP1$) and n 4 ($INP2$) evoke reverberatory activity in dynamic memories [n 1 – n 2] or [n 5 – n 6] respectively and activate the appropriate neuroid in the inhibitory block (n 10 or n 9 respectively) These inhibitory neuroids in turn inhibit the activity of the opposite side of the network ("capturing" the time window)

The reverberating activity in [n 1 – n 2] or [n 5 – n 6] continuously stimulates the corresponding output neuroid with subthreshold intensity If this continuous subthreshold stimulation meets the spike transmitted directly from the input, the corresponding output neuroid is activated

Simulation experiments

The same input frequencies, starting simultaneously

The situation can be described with $D = 0$ ms ($SP_0^{(1)} = SP_0^{(2)}$) and $I^{(1)} = I^{(2)}$ (Fig 1Cb)

The simulation results are demonstrated in Fig 3 in the form of a raster map The considered part of simulation started at 360 ms and ended at 600 ms of simulation time The input frequencies (records $i1$, $i2$) were $F^{(1)} = F^{(2)} \sim 66$ Hz ($I^{(1)} = I^{(2)} = 15$ ms) The network activity was governed by the coincidence detector (n 8) activated at the start of this part of simulation (360 ms), which then gradually inhibited the dynamic memories [n 1 – n 2], [n 5 – n 6] (360–400 ms) and finally (from 400 ms) blocked them completely

The output neuroids (nn 3, 7) continuously received subthreshold excitatory influence (not shown) from $INP1, INP2$ but there was no output from the network since the dynamic memories were inactive

The same input frequencies, starting non-simultaneously

If two same input frequencies differ in the arrival time of the first spike and their inter-spike intervals are equal, the situation can be described with $D \neq 0$ ms ($SP_0^{(1)} \neq SP_0^{(2)}$) and $I^{(1)} = I^{(2)}$ (Fig 1Cb)

In this case the opposite sides of the network alternate in mutual inhibition The situation is illustrated in Fig 3 (considered part of simulation started at 5 ms and ended at 220 ms of simulation time when $F^{(2)}$ was switched off) The input frequencies (records $i1$, $i2$) were $F^{(1)} = F^{(2)} \sim 66$ Hz ($I^{(1)} = I^{(2)} = 15$ ms) with $D = 7\,5$ ms

The inhibitory activity of n 10 (mediated by path $INP1 – n\,0 – n\,10 – nn\,5,6$) alternated with the inhibitory activity of n 9 (path $INP2 – n\,4 – n\,9 – nn\,1,2$) The

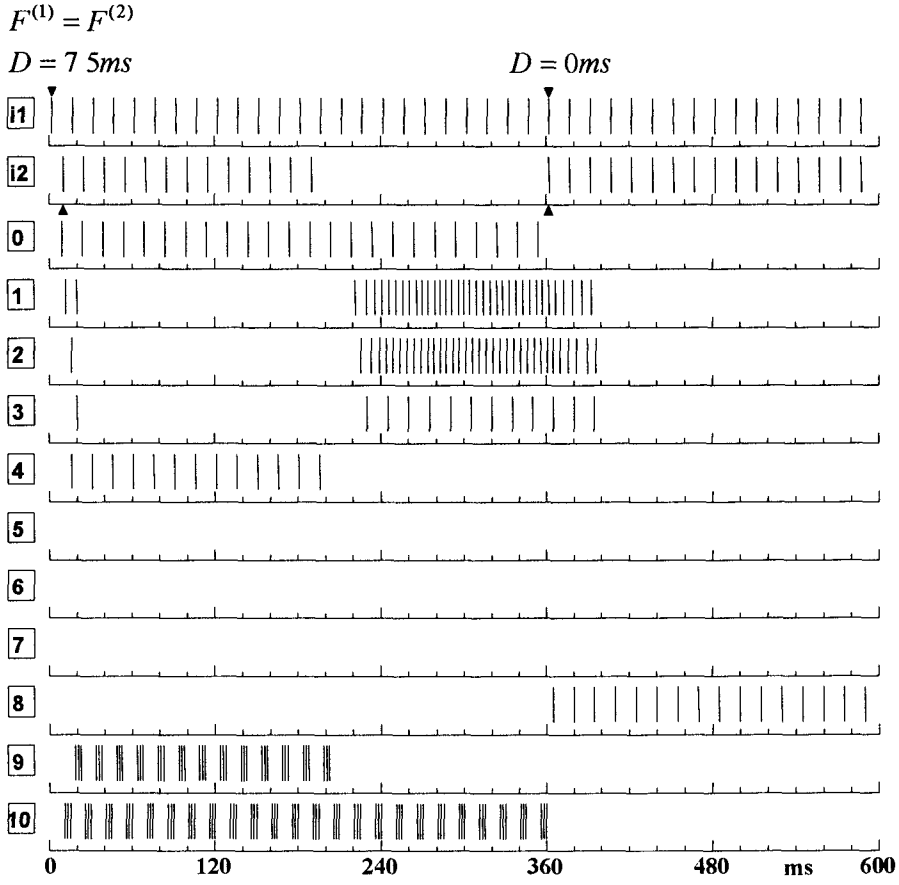

Figure 3. The activity in the network (Fig 2A) during processing of equal frequencies The raster maps of both inputs ($i1$, $i2$) with frequencies $F^{(1)}$, $F^{(2)}$ and all neuroids (0–10) are shown Simulation time was 600 ms The values used in the simulation were $I^{(1)} = I^{(2)} = 15$ ms ($F^{(1)} = F^{(2)} \sim 66$ Hz) At the beginning of the simulation the start of $F^{(2)}$ was slightly delayed ($D = 7\ 5$ ms) (black triangles on the left side) After 200 ms of simulation time $F^{(2)}$ was switched off At 360 ms of simulation time $F^{(2)}$ was switched on again but this time simultaneously ($D = 0$ ms) with $F^{(1)}$ (black triangles on the right)

stimulation of both output neuroids ($n.3/n.7$) was continuous but subthreshold (not shown); as the dynamic memories were inactive (inhibited by $nn.9, 10$) no output signals were generated.

Different input frequencies

In both previous situations the input frequencies were the same, i.e. $I^{(1)} = I^{(2)}$. In general no special values of D, $I^{(1)}$ and $I^{(2)}$ have to be assumed (Fig. 4, Fig. 5, Fig. 6, Fig 8).

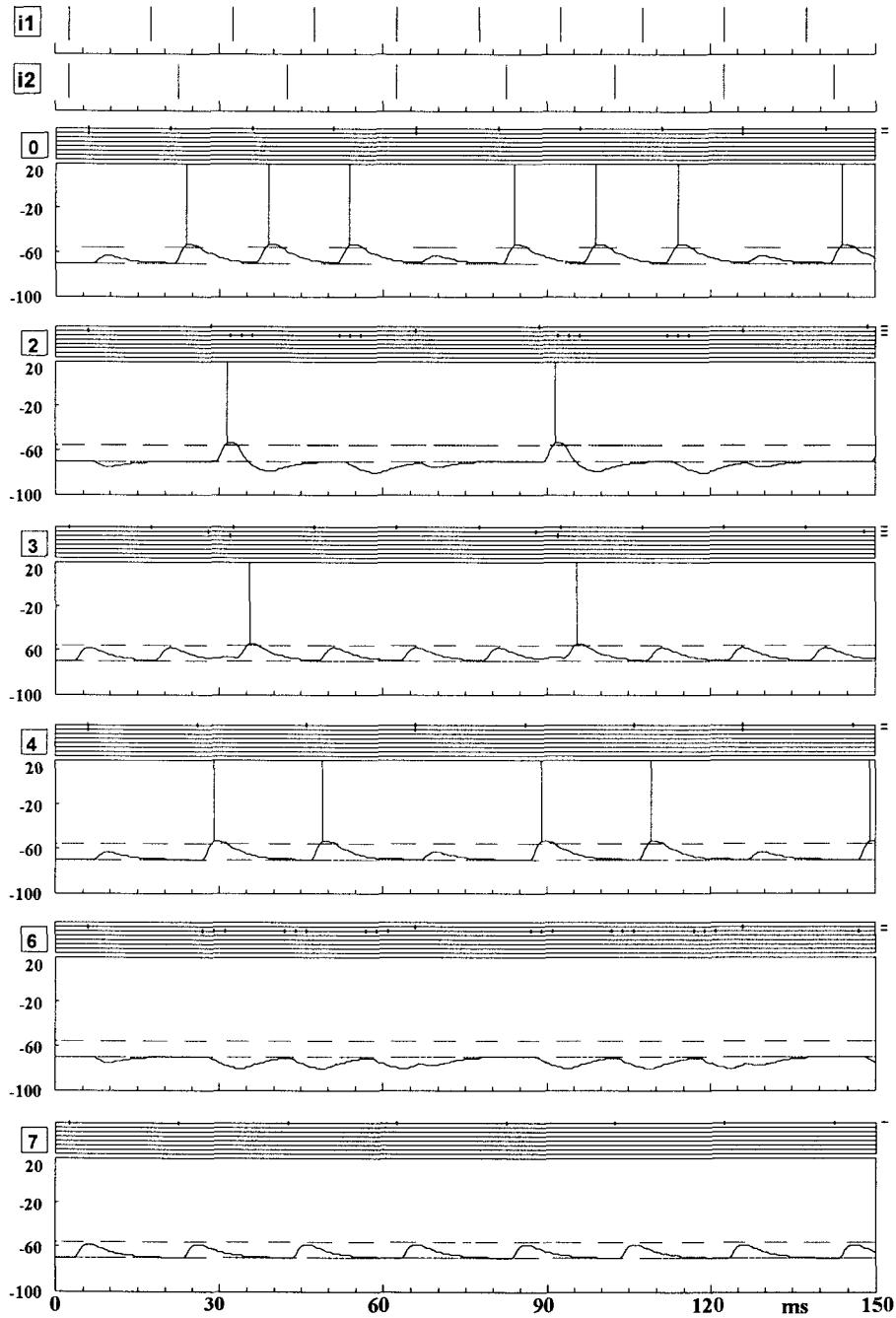
i1
i2
0
20
-20
-60
-100
2
20
-20
-60
-100
3
20
-20
60
-100
4
20
-20
-60
-100
6
20
-20
-60
-100
7
20
-20
-60
-100
0
30
60
90
120
ms
150

The results of simulation experiment, with different input frequencies ($F^{(1)} \sim$ 66 Hz, $I^{(1)} = 15$ ms and $F^{(2)} = 50$ Hz, $I^{(2)} = 20$ ms) starting simultaneously, are shown in Figs. 4, 5. Both inputs (records $i1$, $i2$) were active from 5 ms till the end of simulation time (150 ms).

The coincidence detecting $n.8$ detected simultaneous input spikes at 5 ms, 65 ms, 125 ms (record 8) and stopped the spiking activity in the network until the next input spike arrival. It is evident how the activity moved from one side of the network to the other one (e.g., $nn.9, 10$) – "capturing the time window". Because the input frequency $F^{(1)}$ was higher than $F^{(2)}$, the $F^{(1)}$ channel succeeded, at 35 ms and 95 ms, in activating of the output neuroid ($n.3$).

The dynamics of processing in the model network is shown in Fig. 6A,B. The input frequencies were not constant but either one or both of them changed during the simulation experiment (empty triangles).

A simulation in which only one input frequency ($F^{(2)}$ entering *via* $INP2$) changed is shown in Fig. 6A. $F^{(1)}$ was constant ($\sim$ 66 Hz, $I^{(1)} = 15$ ms) and $F^{(2)}$ decreased from $\sim$ 33 Hz to 25 Hz ($I^{(1)}$ from 30 ms to 40 ms) at 315 ms. As $F^{(1)}$ was still higher than $F^{(2)}$ the output $n.3$ was active during the whole simulation; the output frequency increased from $\sim$ 33 Hz to $\sim$ 46 Hz and changed its pattern. The output $n.7$ remained inactive.

Both inputs were allowed to change in simulation depicted in Fig. 6B. At the beginning of simulation $F^{(1)}$ and $F^{(2)}$ were 100 Hz ($I^{(1)} = 10$ ms) and $\sim$ 66 Hz ($I^{(2)} = 15$ ms) respectively. At 315 ms of simulation time $F^{(1)}$ decreased to 50 Hz ($I^{(1)} = 20$ ms), and at 300 ms of simulation time $F^{(2)}$ decreased to 40 Hz ($I^{(2)} = 25$ ms) (empty triangles). The only active output neuroid was $n.3$ since $F^{(1)}$ was still higher than $F^{(2)}$; the output frequency decreased from $\sim$ 33 Hz to $\sim$ 10 Hz as a result of input frequency change. The output $n.7$ remained inactive.

Differences in input frequencies detectable by the model network

Three situations of processing frequencies with *different* inter-spike intervals are

Figure 4. The activity flow in the model network (Fig. 2A) using simultaneously starting ($D = 0$ ms) input frequencies $F^{(1)} \sim 66$ Hz ($I^{(1)} = 15$ ms) and $F^{(2)} = 50$ Hz ($I^{(1)} = 20$ ms). All records share the same time scale (bottom) – 5-ms divisions, 150 ms the whole simulation time. The raster maps $i1$, $i2$ (vertical bars mark the occurrence of spikes) are records of the two inputs entering the model network. The records below the raster maps show the results of simulating the intracellularly recorded post synaptic potentials in neuroids 0, 2, 3, 4, 6 and 7 The eight horizontal lines above the simulated recordings represent possible synaptic inputs, and the small vertical bars superimposed on them indicate spikes arriving at the synaptic ending (active inputs are marked by short horizontal bars on the right hand side). The upper (dotted) horizontal lines are the threshold levels for spike generation (vertical bars on the simulated recordings). The lower (dash-dot-dot) horizontal lines represent resting transmembrane potential. Abscissa, simulation time in milliseconds; ordinate, simulation of the transmembrane potential in millivolts.

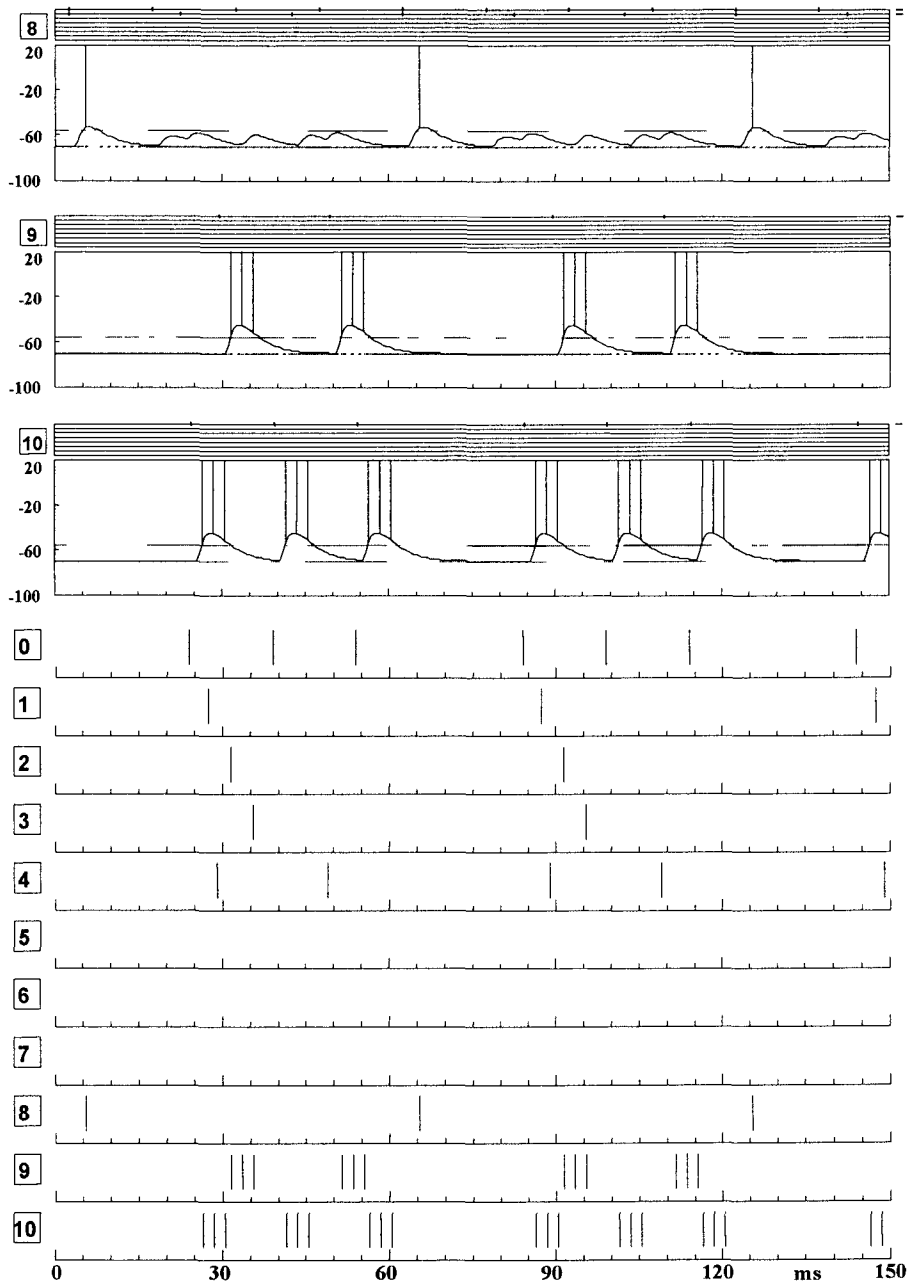

Figure 5. The activity flow in the model network (Fig. 2A) For detailed description, see Fig. 4. The simulations of intracellular recordings of activity of neuroids 8, 9, 10 are shown in the upper part. The raster map in the lower part shows the activity of all 11 neuroids of the network during the simulation.

depicted in Fig. 7. In the first case (part a) $I^{(1)} = 15$ ms ($F^{(1)} \sim 66$ Hz), $I^{(2)} = 17.5$ ms ($F^{(2)} \sim 57$ Hz) which makes the inter-spike interval difference $\Delta I = 2.5$ ms. This difference was detected and the output $n.3$ generated spiking activity with frequency of ~ 10 Hz.

The inter-spike interval difference of 2 ms ($I^{(1)} = 15$ ms, $F^{(1)} \sim 66$ Hz, $I^{(2)} = 17$ ms, $F^{(2)} \sim 59$ Hz) was still detectable (part b) and $n.3$ was active although the output spiking frequency was considerably lower (~ 4 Hz).

The inter-spike interval difference of 1.5 ms ($I^{(1)} = 15$ ms, $F^{(1)} \sim 66$ Hz, $I^{(2)} = 16.5$ ms, $F^{(2)} \sim 60$ Hz) was not detected (part c) and $n.3$ remained silent.

As the inter-spike intervals of the different input frequencies approached each other, the output frequency slowed down; in fact $\Delta I = 2$ ms was the smallest difference detectable by the model network using the input frequencies in the range 40–70 Hz.

Changes in output frequency in relation to changes in input frequencies

To study the relation between the input and output frequencies three types of simulation experiments were made. In this section $F^{(3)}$ denotes the (mean) output frequency counted after 1000 ms of simulation time.

In the first case the higher input frequency ($F^{(1)}$) was constant (~ 66 Hz; $I^{(1)} = 15$ ms) and the lower one ($F^{(2)}$) changed from ~ 50 Hz to ~ 16 Hz ($I^{(2)}$ from 20 ms to 60 ms in 5-ms steps). The results of simulation experiments are summarized in Fig 6C. The relation between $F^{(3)}/F^{(1)}$ and inter-spike interval difference ΔI is shown. The results show that – if the higher input frequency is constant – the (mean) output frequency ($F^{(3)}$) is proportional to ΔI. This proportionality was preserved also when the *higher* frequency was changing and the lower one was constant (not shown).

In the second case both input frequencies were changing but the inter-spike interval difference (ΔI) remained constant. $F^{(1)}$ changed from 100 Hz to 20 Hz ($I^{(1)}$ from 10 ms to 50 ms in 5 ms steps) and $F^{(2)}$ changed from 66 Hz to 18 Hz ($I^{(2)}$ from 15 ms to 55 ms in 5 ms steps). The results of simulations in which $\Delta I = 5$ ms are depicted in Fig. 6D. The relation between $F^{(3)}/F^{(1)}$ and $I^{(1)}$ ($I^{(2)}$) was found to be approximately exponential.

In the third case the ratio $I^{(1)}/I^{(2)}$ was constant and $F^{(1)}$ was higher than $F^{(2)}$. The input frequencies were in the 29–100 Hz range. Seven different $I^{(1)}/I^{(2)}$ ratios were examined: 1/3, 2/5, 1/2, 3/5, 2/3, 3/4 and 4/5. The results of simulations in which $I^{(1)}/I^{(2)}$ ratios were 2/3, 3/4 and 4/5 are shown in Fig. 8B, panels d, e, f respectively. $F^{(3)}/F^{(1)}$ was approximately constant in all cases, i.e. the output frequency ($F^{(3)}$) rose with the increasing higher input frequency ($F^{(1)}$) to keep the $F^{(3)}/F^{(1)}$ ratio constant. Moreover, the constant $F^{(3)}/F^{(1)}$ ratio was higher ($F^{(3)}$ value was closer to $F^{(1)}$) with the decreasing $I^{(1)}/I^{(2)}$ ratio (increasing $F^{(1)}/F^{(2)}$ ratio).

All relations among the output and input frequencies mentioned are fits to the results of simulations. The occasionally occurring values which did not correspond well to these fits (Fig. 6C,D; Fig. 8Bd,e,f) are discussed below.

Discussion

The importance of rate code

The idea that mean firing rates are used for encoding of stimulus parameters was first developed by Adrian (1926, 1941) who showed that the firing rate of stretch receptor in muscle increases as the static force applied to the muscle increases Further experimental work confirmed the importance of rate code for information processing in the central nervous system (Mountcastle 1957; Mountcastle et al 1990; Hsiao et al. 1993; Johnson and Hsiao 1994). For example, amplitude and phase of sound waves in auditory nerve (barn owl) are rate encoded (Konishi 1991).

The concept of rate code became a standard tool for describing the properties of many types of neurons (see, for example Hubel and Wiesel 1959; Girman et al. 1999; Ramachandran et al. 1999) although it is now subject of debate (see, for example Bialek et al. 1991; Rieke et al. 1997) and is considered to be too simple for brain activity description (Gerstner 1999).

Figure 6. Changes in input frequencies during the simulation *(A, B)* and proposed relations among the input and output frequencies (*C, D*) in the model network (Fig 2A) $F^{(1)}$, $F^{(2)}$ denote the input frequencies, $F^{(3)}$ denotes the output frequency, $I^{(1)}$, $I^{(2)}$ denote the inter-spike interval lengths, ΔI is the inter-spike interval difference between $F^{(1)}$ and $F^{(2)}$ (see *Notation and conventions* for details) **A.** Simulations of intracellular recordings of activity of output neuroids 3, 7 (Fig 2A) are shown Both frequencies started simultaneously (black triangles) – $F^{(1)} \sim 66$ Hz, $I^{(1)} = 15$ ms, $F^{(2)} \sim 33$ Hz, $I^{(1)} = 30$ ms – and $F^{(2)}$ changed its value to 25 Hz ($I^{(2)} = 40$ ms) during the simulation (empty triangles) As a result, the output of neuroid 3 changed **B.** Simulations of intracellular recordings of activity of output neuroids 3, 7 are shown Both frequencies started simultaneously (black triangles) – $F^{(1)} = 100$ Hz, $I^{(1)} = 10$ ms, $F^{(2)} \sim 66$ Hz, $I^{(1)} = 15$ ms – and during the simulation $F^{(1)}$ changed its value to 50 Hz ($I^{(1)} = 20$ ms) and $F^{(2)}$ changed its value to 40 Hz ($I^{(2)} = 25$ ms) (empty triangles) As a result of this change the output of neuroid 3 changed **C.** Results of simulations in which the higher input frequency ($F^{(1)}$) was constant (~ 66 Hz, $I^{(1)} = 15$ ms) A proposed relation between $F^{(3)}/F^{(1)}$ and ΔI is shown Crosses mark the results of particular simulations, the black and empty triangles correspond to the triangles in part A of this Figure The straight line, showing the proposed relation, is a linear regression fit to the results **D.** Results of simulations in which ΔI was constant ($\Delta I = 5$ ms) A proposed relation between $F^{(3)}/F^{(1)}$ and $I^{(1)}$ is shown Note that, since ΔI is constant, there is an analogical relation between $F^{(3)}/F^{(1)}$ and $I^{(2)}$ Crosses mark the results of particular simulations, the black and empty triangles correspond to the triangles in part B of this Figure The proposed exponential relation is the best fit to the results
Note $F^{(1)}$ is higher in all simulations considered in this Figure, which means that the only output frequency is $F^{(3)}$

"Reading" the rate code

The basic idea of rate coding is that most of the relevant information is contained in the mean firing rate of the neuron. However, there are at least three different

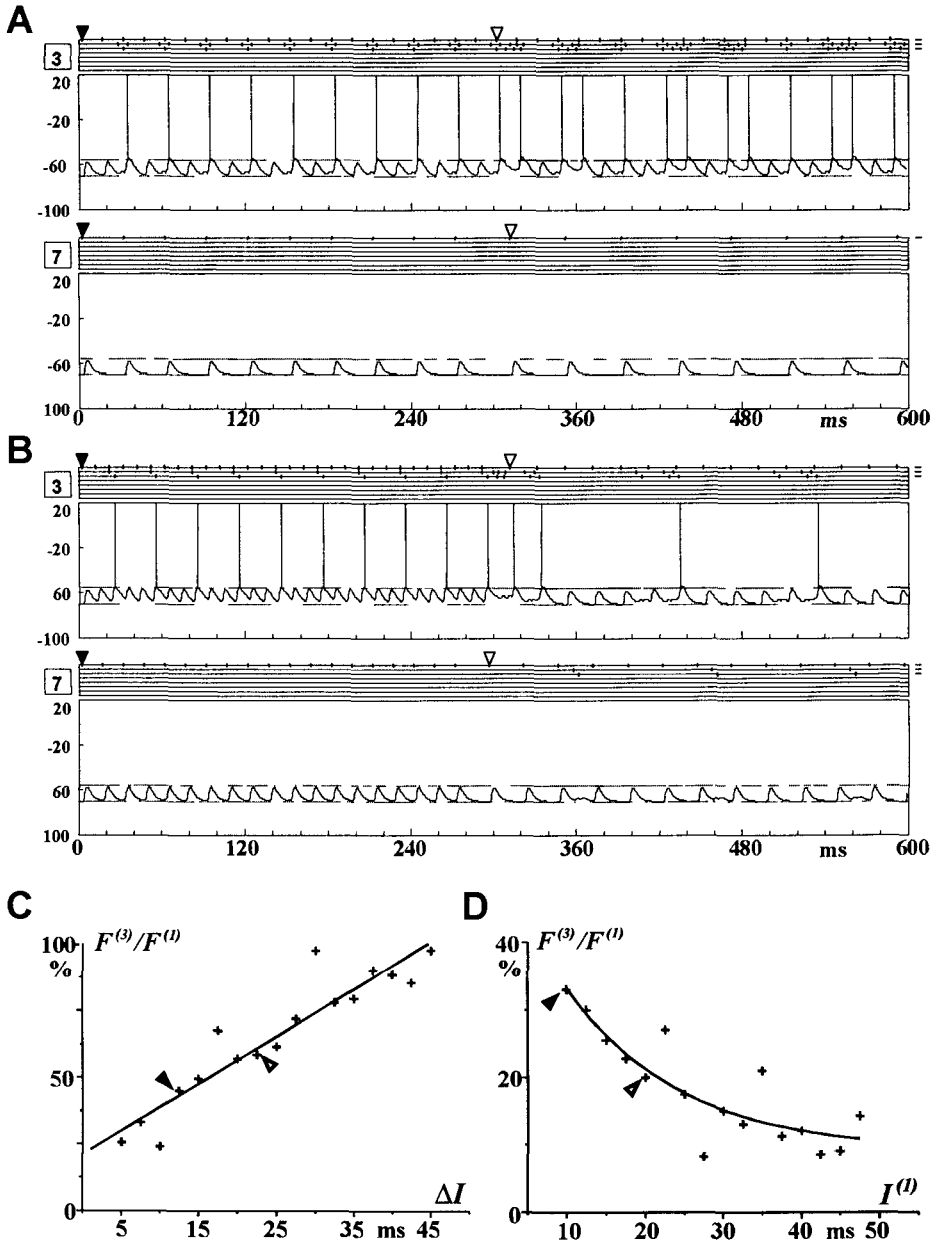

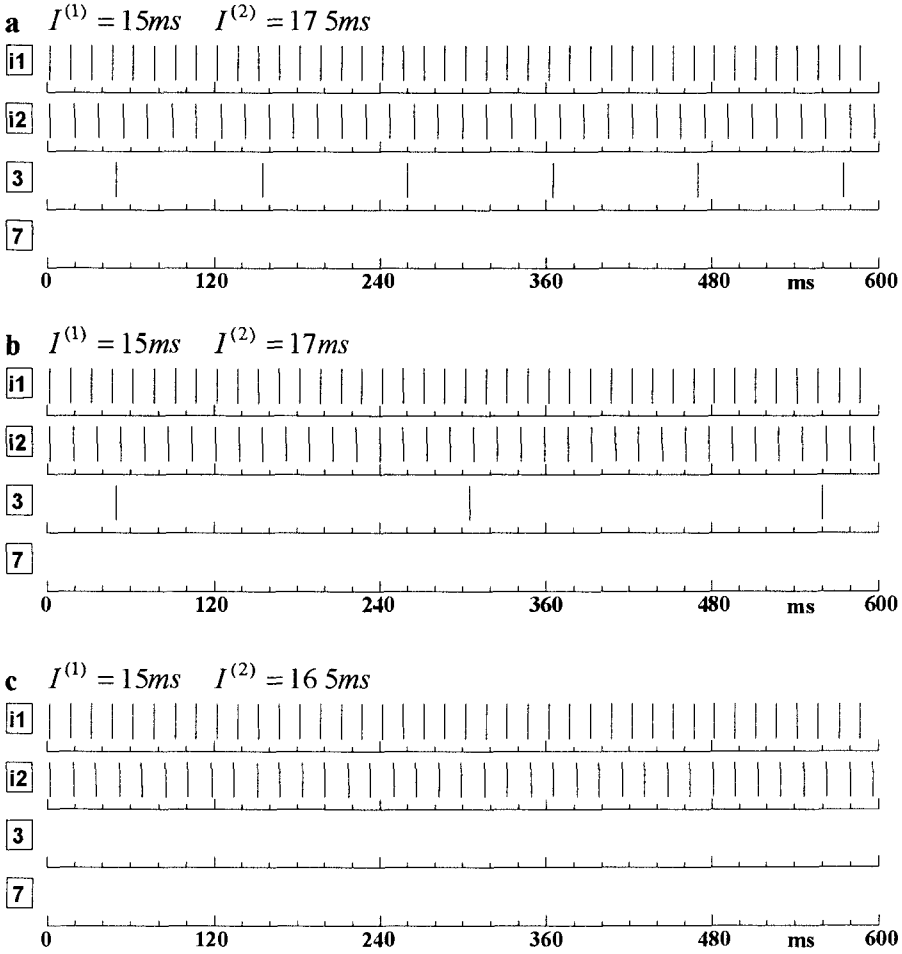

Figure 7. Differences in input frequencies detectable by the model network (Fig 2A) The raster maps of the two inputs $i1$, $i2$ and output neuroids 3, 7 are shown The input frequencies started simultaneously The time scale is 600 ms ΔI denotes the difference in the lengths of inter-spike intervals ($\Delta I = |I^{(1)} - I^{(2)}|$) a) $I^{(1)} = 15$ ms ($F^{(1)} \sim 66$ Hz), $I^{(2)} = 17\,5$ ms ($F^{(2)} \sim 57$ Hz), $\Delta I = 2\,5$ ms, b) $I^{(1)} = 15$ ms ($F^{(1)} \sim 66$ Hz), $I^{(2)} = 17$ ms ($F^{(2)} \sim 59$ Hz), $\Delta I = 2$ ms, c) $I^{(1)} = 15$ ms ($F^{(1)} \sim 66$ Hz), $I^{(2)} = 16\,5$ ms ($F^{(2)} \sim 60$ Hz), $\Delta I = 1\,5$ ms See text for details

notions of (mean firing) rate which are often confused (Gerstner 1999): an average over time, an average over several neurons or an average over several runs of an experiment. The temporal average (Adrian 1926) – simplest and most commonly used notion of firing rate – is also used in this paper. This is essentially the spike count inside a given time window divided by the length of this time window.

To exploit the information contained in rate-encoded spike trains, for example the discharge from the slowly adapting peripheral afferents (Zigmond et al 1999), the central nervous system continuously has to monitor, analyze and compare its inputs entering along parallel lines

To obtain a rate-encoded information incoming along just one fiber it would be enough to determine the number of spikes during the given time window With the assumption of regular input frequency, as it is in our paper, it is enough to compute the length of just one inter-spike interval to obtain the frequency value

It is not necessary to determine the inter-spike interval lengths if the nervous system only needs to *compare* the incoming rate-encoded spike trains In such a case a comparison of corresponding inter-spike intervals (Pavlásek et al 1996) suffices, which is exactly the problem presented in this paper

The proposed model network is able to continuously compare incoming frequencies (rate-encoded spike trains) and dynamically change its output according to input changes

Biological plausibility of the model network

The morphological and functional properties of the devised network (e g , convergence or divergence, coincidence detection, delay lines) are so widespread in the nervous system that it is easy to imagine their potential use at any level of information processing

The input frequencies were assumed to be regular, which means that inside an appropriate time window the interspike interval lengths were constant The time window cannot be made arbitrarily short because the processing of an input requires some time (for example, Fig 3, n 3, from 360 ms to 400 ms of simulation time) and, moreover, when using very short time windows, the distinction between rate code and temporal code is not clear (Theunissen and Miller 1995)

Regular frequencies occur in the nervous system and many isolated neurons generate approximately regular sequences of spikes when injected a constant current (Jack et al 1975, McCormick et al 1985, Mainen and Sejnowski 1995)

Network parameters

Four basic parameters of the neuroids and their connections were adjusted in order to establish the proper dynamics of the network shape of the post-synaptic potential (*Psp*), threshold (*Th*) value, synaptic weight value (*Sw*) and delay lines

To simplify the design and analysis of the network, *Psp* shape and *Th* values were chosen to be the same for all neuroids

The specific parameters of *Psp* (see *Methods*) were set according to the experimental results, so that the *Psp* time course (Fig 2B) would resemble the time course of experimental results as close as possible Changing any of the parameters (t_1, t_2) would require further adjustment of the other parameters of neuroids The relative threshold values were set at 0 5 for all neuroids

Both delay lines (Fig 2A) were designed specifically ($delay$ = 3 5 ms) to allow n 8 to inhibit the rest of neuroids after detecting coincident spikes

Having these parameters constant it was the value of synaptic weight that had to be adjusted in order to set the proper behaviour of the network. Three main types of weight values were used. All neuroids with suprathreshold excitatory influence had their synaptic weights ($Sw = 0.6$) set above the Th value. The synaptic weights of inhibitory neuroids ($Sw = -0.7$) were set to be opposite in value to their excitatory counterparts. Both subthreshold excitatory inputs of $n.8$

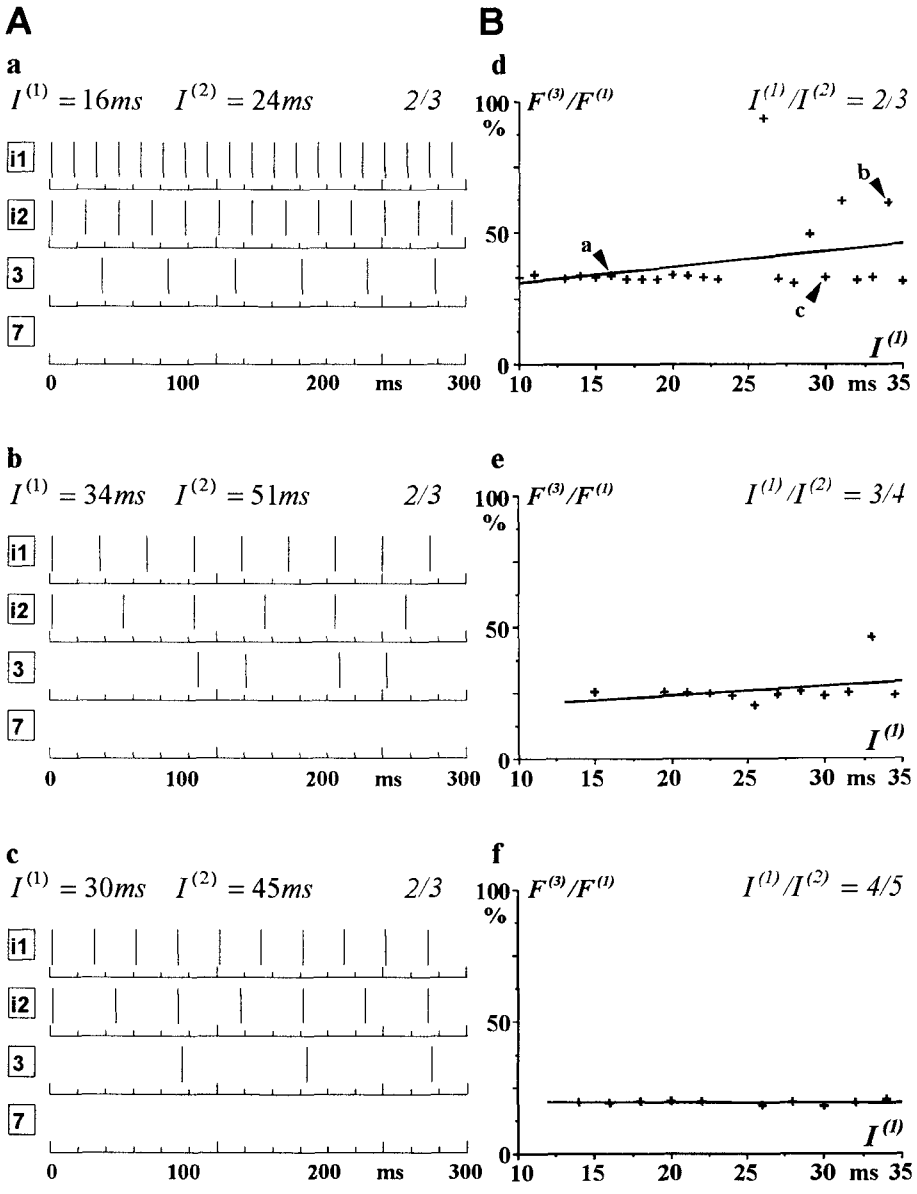

were set at 0.6 Th ($Sw = 0\ 3$) in order to enable the proper coincidence detection. Subthreshold excitatory inputs of $nn.3, 7$ were set in the following way. inputs from dynamic memories [1; 2], [5; 6] had small synaptic weights ($Sw = 0.085$) and the inputs incoming directly from the input lines were slightly subthreshold ($Sw = 0.4$). Therefore weak, continuous stimulation from dynamic memories required strong influence from input lines in order to generate a spike at the output

The network parameters were chosen specifically to enable the network to perform the task. Change in any of the above parameters would require appropriate adjustments of the other parameters in order to re-establish the proper network dynamics.

"Coding" properties of the network

In the definition of the presented problem we assumed that the network only detects the difference between the input frequencies. However, according to results of simulation experiments it can be assumed that the (mean) output frequency value is influenced by the input frequencies.

In the first case if $F^{(1)}$ is constant (and higher than $F^{(2)}$) and $F^{(2)}$ is gradually slowing down then more and more spikes of $F^{(1)}$ occur between the spikes of $F^{(2)}$ (simply because $I^{(2)}$ is progressively longer than $I^{(1)}$). If the lower input frequency is constant and the higher one is changing the situation is analogical The resulting (mean) output frequency is proportional to ΔI (inter-spike interval difference), the faster the constant frequency the steeper the dependence

The second case (constant ΔI) is more complex Both input frequencies gradually slow down ($I^{(1)}$ and $I^{(2)}$ rise) and due to constant ΔI the ratio $I^{(1)}/I^{(2)}$ approaches 1 According to network definition this must mean that the resulting output frequency will gradually slow down so the ratio $F^{(3)}/F^{(1)}$ will approach 0

Figure 8. Results of simulations (network – Fig 2A) with a constant $I^{(1)}/I^{(2)}$ ratio (the actual values of input frequencies vary) $F^{(1)}$, $F^{(2)}$ denote the input frequencies, $F^{(3)}$ denotes the output frequency, $I^{(1)}$, $I^{(2)}$ denote the inter-spike interval lengths (see *Notation and conventions* for details) **A.** The results of simulations with $I^{(1)}/I^{(2)} = 2/3$ Raster maps of the two input frequencies ($i1$, $i2$) and output neuroids (3, 7) are shown Both input frequencies started simultaneously Simulation time was 300 ms The values of $I^{(1)}$ ($F^{(1)}$) and $I^{(2)}$ ($F^{(2)}$) were as follows a) $I^{(1)} = 16$ ms ($F^{(1)} \sim 62$ Hz), $I^{(2)} = 24$ ms ($F^{(2)} \sim 42$ Hz), b) $I^{(1)} = 34$ ms ($F^{(1)} \sim 29$ Hz), $I^{(2)} = 51$ ms ($F^{(2)} \sim 20$ Hz), c) $I^{(1)} = 30$ ms ($F^{(1)} \sim 33$ Hz), $I^{(2)} = 45$ ms ($F^{(2)} \sim 22$ Hz) **B.** The results of simulations with three different $I^{(1)}/I^{(2)}$ ratios The proposed relations between $F^{(3)}/F^{(1)}$ and $I^{(1)}$ are shown Crosses mark the results of particular simulations The straight lines, showing the proposed relations, are linear regression fits to the results d) $I^{(1)}/I^{(2)} = 2/3$ The black triangles marked a, b, c correspond to panels *a, b, c* of this Figure e) $I^{(1)}/I^{(2)} = 3/4$, f) $I^{(1)}/I^{(2)} = 4/5$

Note $F^{(1)}$ is higher in all simulations considered in this Figure, which means that the only output frequency is $F^{(3)}$

And finally, in the third case (constant $I^{(1)}/I^{(2)}$) it is evident that the *relative* position of spikes in input frequencies and then the relative position of spikes during processing in the network (we assumed regular frequencies) is constant and only the *absolute* lengths of $I^{(1)}$ and $I^{(2)}$ differ Consequently the output generated by the network is (in principle) the same The only difference is the time scale of the output the faster the input frequencies the faster the output frequency This means that also position of spikes in the output train related to the position of spikes in the faster input frequency is constant and the ratio $F^{(3)}/F^{(1)}$ (in our case) must be constant

The proposed relations among input and output frequencies are fits to the results of simulation experiments Some of the results are not in agreement with the predicted values (see, for example, Fig 8Bd and Fig 8Be) These results represent the situations in which the *output pattern changed* (see Fig 6A, Fig 8Ab) However, such outlaid values are allowed because the network was designed to *compare* the input frequencies and the results of simulations do tell us which frequency is higher

On the other hand, the results do suggest that the network could encode the information about both input frequencies into one output stream But the proper encoding would require a well-tuned network with precise values of neuroid parameters, it is an open question whether such precise parameter values would be attainable in real neuronal networks

The output stream would then encode both the position of higher frequency (location code) and the relation between the input frequencies (mean rate code) However, in order to exploit these types of information contained in output stream the decoding mechanism should know what the original frequency was

Biological reality solving more complex tasks

Comparing only two regular incoming frequencies is certainly a simplified case The central nervous system faces a fairly more difficult task It needs to compare many different frequencies entering along thousands of parallel fibers The proposed model network is small and simple and many of such small "comparators" would have to be combined together (in parallel) for continuous monitoring of the incoming frequencies for the processing in the higher stages of the nervous system

It is virtually impossible to compare every couple made of various inputs incoming from the whole body because such comparison would require an enormous amount of comparators The required amount would grow exponentially with the growing number of inputs

We can assume that only the inputs incoming from *adjacent* places are considered to be relevant for frequency comparison and as such they are compared For example, the code for roughness exists in the difference in firing rates between *adjacent* slowly adapting Type I (SAI) afferents (Hsiao et al 1993)

Further reduction of the required amount of comparators can be obtained if we assume that the *exact* comparison of inputs from two adjacent *points* (i e two adjacent receptors) is not important for information processing in higher stages but only rough difference detection (i e lower *vs* higher) between larger (macroscopic)

areas is required. For example, the minimum separation between two points that permits each to be perceived separately (two-pointlimen) around the mouth is 0 5 mm, but the Merkel disks density in the same region is 50 mm^{-2} (Zigmond et al. 1999)

It is hypothessed, that in such a case, the continuous difference detection of inputs incoming from adjacent receptor areas (e.g., edge detection) might be effected in a stepwise manner. The presented network(s) could be connected in a few successive steps, first selecting the fastest frequency in the areas and then comparing the "winners" together.

These assumptions correspond well with neurophysiological findings that the receptive fields of neurons in somatosensory system tend to become larger at higher levels as the contributions from a large number of receptors are added and compared with one another (Zigmond et al. 1999).

References

Adrian E D (1926) The impulses produced by sensory nerve endings J Physiol (London) **61**, 49—72

Adrian E D (1941) Afferent discharges to the cerebral cortex from peripheral sense organs J Physiol **100**, 159—191

Bialek W , Rieke F , de Ruyter van Steveninck R , Warland D (1991) Reading a neural code Science **252**, 1854—1857

Gerstner W (1999) Spiking Neurons In Pulsed Neural Networks (Eds W Maas and C M Bishop), pp 3—53, MIT Press, Cambridge, MA

Gerstner W , Kreiter A K , Markram H , Herz A V M (1997) Neural codes firing rates and beyond Proc Natl Acad Sci U S A **94**, 12740—12741

Girman S V , Sauvé Y , Lund R D (1999) Receptive field properties of single neurons in rat primary visual cortex J Neurophysiol **82**, 301—311

Hernández A , Zainos A , Romo R (2000) Neuronal correlates of sensory discrimination in the somatosensory cortex Proc Natl Acad Sci U S A **97**, 6191—6196

Hsiao S S , Johnson K O , and Twombly I A (1993) Roughness coding in the somatosensory system Acta Psychol **84**, 53—67

Hubel D H , Wiesel T N (1959) Receptive fields of single neurons in the cat's striate cortex J Physiol (London) **148**, 574—591

Jack J J B , Noble D , Tsien R W (1975) Electric Current Flow in Excitable Cells Clarendon Press, Oxford

Jančo J , Stavrovský I , and Pavlásek J (1994) Modeling of neuronal functions a neuron-like element with the graded response Comput Artif Intellig **13**, 603—620

Johnson K O , Hsiao S S (1994) Evaluation of the relative roles of slowly and rapidly adapting afferent fibres in roughness perception Can J Physiol Pharmacol **72**, 488—497

Konishi M (1991) Similar algorithms in different sensory systems and animals In The Brain, volume LV of Cold Spring Harbor Symposia on Quantitative Biology, pp 575—584, Cold Spring Harbor Laboratory Press, New York

Mainen Z F , Sejnowski T J (1995) Reliability of spike timing in neocortical neurons Science **268**, 1503—1506

McClurkin J W , Optican L M , Richmond B J , Gawne T J (1991) Concurrent processing and complexity of temporally encoded neuronal messages in visual perception Science **253**, 675—677

McCormick D A , Connors B W , Lighthall J W , Prince D A (1985) Comparative electrophysiology of pyramidal and sparsely spiny stellate neurons of the neocortex J Neurophysiol **54**, 782—806

Mountcastle V B (1957) Modality and topographic properties of single neurons of cat's somatosensory cortex J Neurophysiol **20**, 408—434

Mountcastle V B , Steinmetz M A , Romo R (1990) Cortical neuronal periodicities and frequency discrimination in the sense of flutter In The Brain, volume LV of Cold Spring Harbor Symposia on Quantitative Biology, pp 861—872, Cold Spring Harbor Laboratory Press, New York

Pavlásek J , Poledna J , Jagla F (1996) Time intervals comparing neural network Neural Networks **9**, 1131—1140

Pavlásek J (1999) Temporal patterns recognized by a network of coordinated time delays and coincidence detectors Gen Physiol Biophys **18**, 249—255

Ramachandran R , Davis K A , May B J (1999) Single-unit responses in the inferior colliculus of decerebrate cats I Classification based on frequency response maps J Neurophysiol **82**, 152—163

Richmond B J , Optican L M , Podel M , Spitzer H (1987) Temporal encoding of two-dimensional patterns by single units in primate inferior temporal cortex I Response characteristics J Neurophysiol **57**, 132—146

Richmond B J , Optican L M , Spitzer H (1990) Temporal encoding of two-dimensional patterns by single units in primate primary visual cortex I Stimulus-response relations J Neurophysiol **64**, 351—369

Rieke F , Warland D , de Ruyter van Steveninck R , Bialek W (1997) Spikes Exploring the Neural Code MIT Press, Cambridge, MA

Theunissen F , Miller J P (1995) Temporal encoding in nervous systems a rigorous definition J Comput Neurosci **2**, 149—162

Willis Jr W D , Coggeshall R E (1991) Sensory Mechanisms of the Spinal Cord Plenum Press, New York, 2nd edition

Zigmond M J , Bloom F E , Landic S C , Roberts J L , Squire L R , editors (1999) Fundamental Neuroscience Academic Press, San Diego

Final version accepted February 8, 2001